Transformer Neural Networks in the Measurement of $t\bar{t}H$ Production in the $H \to b\bar{b}$ Decay Channel with ATLAS

Chris Scheulen[1]$\star$, on behalf of the ATLAS Collaboration

1 Université de Genève, Geneva, Switzerland

$\star$ chris.scheulen@cern.ch

Abstract

A measurement of Higgs boson production in association with a top quark pair in the bottom–anti-bottom Higgs boson decay channel and leptonic top final states is presented. The analysis uses 140 fb^{-1} of 13 TeV proton–proton collision data collected by the ATLAS detector at the Large Hadron Collider. A particular focus is placed on the role played by transformer neural networks in discriminating signal and background processes via multi-class discriminants and in reconstructing the Higgs boson transverse momentum. These powerful multi-variate analysis techniques significantly improve the analysis over a previous measurement using the same dataset.

1 Introduction

The Yukawa coupling of the top quark – the heaviest particle in the Standard Model – to the Higgs boson is suspected to play a critical role in electroweak symmetry breaking and the stability of the Higgs vacuum potential. While the coupling can be measured indirectly from the quantum loops underpinning the effective Higgs boson couplings to gluons and photons, its direct measurement is only feasible in processes involving the associated production of Higgs bosons and top quarks.

In this context, the ATLAS collaboration [1] at the Large Hadron Collider [2] recently published a measurement [3] of the associated production of a top quark pair with a Higgs boson ($t\bar{t}H$) in the bottom–anti-bottom Higgs boson decay channel ($H \to b\bar{b}$) with the full Run 2 dataset encompassing 140 fb^{-1} of proton–proton collision data collected between 2015 and 2018. $t\bar{t}H$ production has been discovered by both the ATLAS [4] and CMS [5] collaborations in 2018 in combination measurements of several Higgs boson decay channels. The $H \to b\bar{b}$ decay channel of $t\bar{t}H$ production – together called $t\bar{t}H(b\bar{b})$ – offers a large branching fraction of 58 % [6] and the possibility to fully reconstruct the Higgs boson four-momentum at the cost of a large irreducible background consisting of top quark pair production in association with

additional – mostly heavy-flavour – jets ($t\bar{t}$ + jets). Full Run 2 analyses of $t\bar{t}H(b\bar{b})$ production have already been conducted by the ATLAS [7] and CMS [8] collaborations with signal strengths of $0.35^{+0.36}_{-0.34}$ and 0.33 ± 0.26, respectively. The recent ATLAS re-analysis superseding Ref. [7] implements several improvements in the calibrated objects, the systematics model, and an overhauled analysis strategy.

As this publication will summarise the analysis strategy and its results, details on many aspects, such as the background and systematics model, will not be outlined for brevity. A detailed account of the entire analysis is published as Ref. [3].
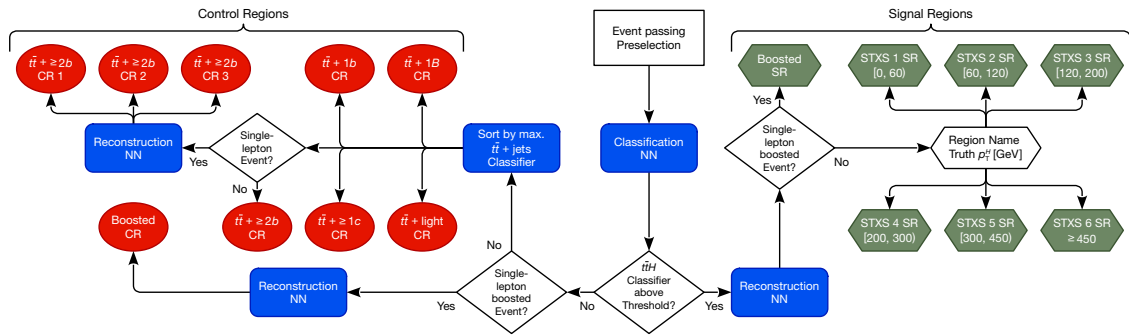
2 Analysis Strategy

Figure 1: Flowchart depicting the multi-variate analysis setup used to assign events into signal and control regions via separate neural networks for event classification and Higgs boson reconstruction. The Figure is taken from Ref. [3].

Following dedicated studies on the dominant $t\bar{t}$ + jets background modelling [9], the background was split up into five separate categories based on the flavour of the jets not originating from top quark decays: $t\bar{t}$ + light and $t\bar{t} + \geq 1c$ only contain additional light and c-jets, respectively. Meanwhile, $t\bar{t} + \geq 1b$ is split into $t\bar{t} + \geq 2b$, $t\bar{t} + 1B$, and $t\bar{t} + 1b$ components corresponding to at least two additional b-jets, one additional jet containing at least two collimated b-hadrons, and one additional jet containing exactly one b-hadron, respectively. Unlike the first full Run 2 analysis, the region definition is entirely based on multi-variate discriminants to allow constraining each $t\bar{t}$ + jets category via a normalisation factor using dedicated control regions as pictured in Figure 1. The $t\bar{t}H$ signal region is additionally split by p_T^H, the Higgs boson transverse momentum, for a differential measurement in the Simplified Template Cross-Section (STXS) formalism [6]. Details on the neural networks used for event categorisation and Higgs boson reconstruction are deferred to the next section.

Thanks to the classification-based region definitions following from the powerful categorisation scheme, the kinematic preselection could be loosened compared to the first full Run 2 analysis, leading to an improvement of the $t\bar{t}H(b\bar{b})$ signal acceptance by a factor of three: events in the single-lepton and dilepton top quark pair decay channels are targeted via kinematic preselections of ≥ 5 jets in association with exactly one lepton (electron or muon), and ≥ 3 jets in association with exactly two leptons, respectively. Because of the b-quarks expected from the decays of the top quarks and the Higgs boson, ≥ 3 b-tags are required in each channel. Additionally, single-lepton events in which both b-quarks from the Higgs boson are contained in a single $\Delta R = 1.0$ jet are selected in a separate boosted channel designed to increase sensitivity at high p_T^H. Simultaneously, these events are vetoed in the single-lepton resolved selection.

3   Transformer Network Performance

The simultaneous measurement of the individual $t\bar{t}$ + jets normalisation factors and the $t\bar{t}H$ signal cross-section is primarily possible because of the sophisticated multi-variate analysis strategy used for event classification and Higgs boson reconstruction. The transformer architecture [10] underlying the neural networks used for classification and reconstruction was originally presented in the context of natural language processing. It is agnostic to the cardinality of input objects and invariant under their permutation. These properties render it especially useful for tasks involving high-energy particle collision events, in which the number of final state particles is variable and where no unambiguous meaningful ordering exists between final state objects. The event classification and Higgs boson reconstruction networks use low-level four-vector and b-tagging information of all jets, leptons, and the missing transverse energy as input variables.

The classification networks predict the most probable event type from among the $t\bar{t}H$ signal and the five $t\bar{t}$ + jets categories introduced in Section 2. In order to use the full information of the multi-class classification probabilities p_i and account for differences between the process yields N_i, the classifiers are converted into six class discriminants d_i as

$$d_i = \frac{p_i}{\sum_{j \neq i} p_j \hat{N}_{ij}}, \qquad \text{where} \quad \hat{N}_{ij} = \frac{N_j}{\sum_{k \neq i} N_k}, \tag{1}$$

corresponding to a ratio of the classifier of the target class i and the average classifier of all other classes j weighted by the corresponding process yield fraction $\hat{N}_{ij}$. In each channel, events are assigned to the signal region based on a $t\bar{t}H$ discriminant threshold optimised to maximise the signal-over-noise ratio $S/\sqrt{B}$. Events not passing this threshold are instead assigned to the control region corresponding to the highest $t\bar{t}$ + jets discriminant value. As the discriminants defined in Equation 1 still show good separation power after the region assignments, the discriminant of each region's corresponding target process was used as the fit variable in the binned profile likelihood fits performed to extract the inclusive and differential $t\bar{t}H$ cross-sections.

The reconstruction networks use a pairing layer operating similarly to the tensor attention layer of SPANet [11] to infer the two most likely jets originating from the Higgs boson decay. The four-vectors of these jets are then combined to reconstruct p_T^H for the differential cross-section measurement. The resulting confusion matrices between the true and the reconstructed p_T^H for the signal events falling in the signal regions are shown in Figure 2. In the boosted channel, the reconstructed p_T^H is used as the fit variable instead of the discriminants used in the other channels.

4   Analysis Results

Good post-fit agreement was observed after a simultaneous binned profile likelihood fit in all regions. Two fit setups were employed to measure both an inclusive $t\bar{t}H$ signal cross-section and a differential p_T^H cross-section in the six STXS bins. The inclusive best-fit cross-section of

$$\sigma_{t\bar{t}H}^{\text{obs}} = 411\,^{+101}_{-\,92}\,\text{fb} = 411 \pm 54\,(\text{stat.})\,^{+85}_{-75}\,(\text{syst.})\,\text{fb}$$

is compatible with the Standard Model prediction of $\sigma_{t\bar{t}H}^{\text{SM}} = 507\,^{+35}_{-50}\,\text{fb}$ [6] at a Higgs boson mass of $m_H = 125.09\,\text{GeV}$. The observed event excess corresponds with a significance of $4.6\,\sigma$ over the background-only hypothesis. The differential cross-section results are shown in Figure 3 with correlation coefficients not exceeding $30\,\%$ and compatibility with the Standard
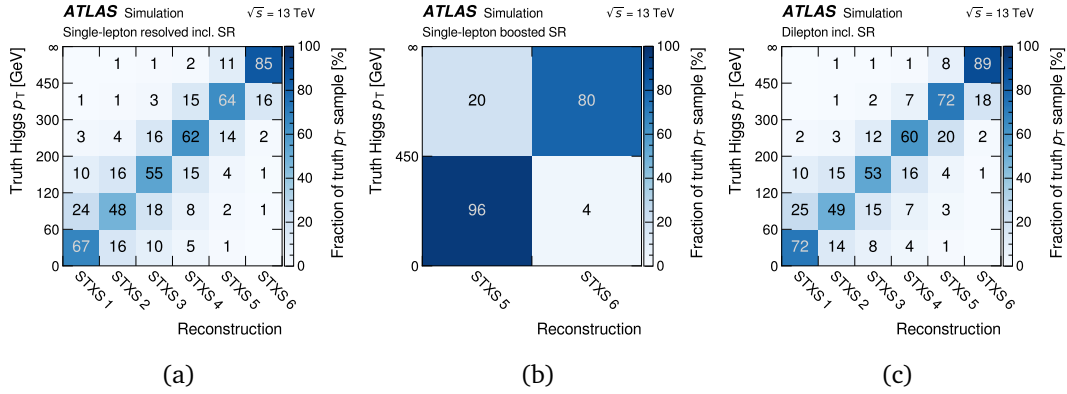
Figure 2: Confusion matrices of the Higgs boson transverse momentum (p_T^H) reconstruction in the signal regions of (a) the single-lepton resolved, (b) the single-lepton boosted, and (c) the dilepton channel. For each truth p_T^H range, the fraction of events assigned to each signal region p_T^H bin is given. The Figures are taken from Ref. [3].
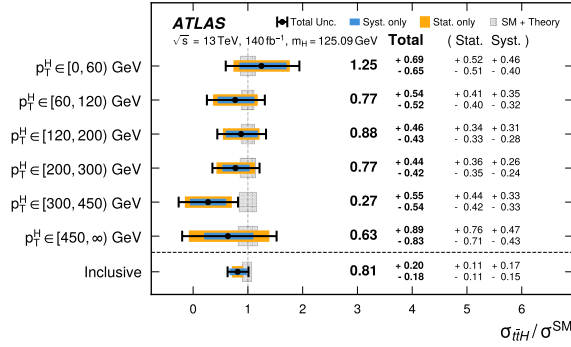

Figure 3: Measurements of the $t\bar{t}H$ cross-section in bins of the truth Higgs boson p_T and inclusively. The Higgs boson rapidity is restricted to $|y_H| \leq 2.5$ for the differential measurement in line with the STXS prescription. Separate uncertainties for measurement and prediction are included. The Figure is taken from Ref. [3].

Model prediction at a p-value of 89 %. Modelling of the $t\bar{t} + \geq 1b$ backgrounds does not constitute the dominant uncertainties, unlike in the first full Run 2 ATLAS analysis. Instead, the $t\bar{t}H$ signal modelling represents the leading sources of systematic uncertainty.

5 Conclusion

A cross-section measurement of Higgs boson associated top quark pair production in the bottom–anti-bottom Higgs boson decay channel using the entire Run 2 proton–proton dataset collected at 13 TeV with the ATLAS detector at the Large Hadron Collider between 2015 and 2018 was presented. It represents a re-analysis of the data incorporating various improvements to the object and systematics model and the analysis strategy. Among these, the utilisation of sophisticated state-of-the-art transformer neural networks for the multi-variate analysis strategy allowed simultaneous measurements of the dominant $t\bar{t}$ + jets background process split into five disjoint categories and the signal process. Additionally, the good event classification performance made it possible to loosen the analysis preselection and increase the signal acceptance by a factor of three compared to the first full Run 2 analysis. The measured signal

cross-section of $\sigma_{t\bar{t}H}^{\text{obs}} = 411\ ^{+101}_{-\ 92}$ fb is compatible with the Standard Model prediction and represents the most precise single-channel $t\bar{t}H$ cross-section measurement to date. An excess of $4.6\,\sigma$ over the background-only hypothesis was observed.

Acknowledgements

References

[1] ATLAS Collaboration, *The ATLAS Experiment at the CERN Large Hadron Collider*, JINST **3**, S08003 (2008), doi:10.1088/1748-0221/3/08/S08003.

[2] L. Evans and P. Bryant (Eds.), *LHC Machine*, JINST **3**, S08001 (2008), doi:10.1088/1748-0221/3/08/S08001.

[3] ATLAS Collaboration, *Measurement of the associated production of a top-antitop-quark pair and a Higgs boson decaying into a $b\bar{b}$ pair in pp collisions at $\sqrt{s} = 13$ TeV using the ATLAS detector at the LHC* (2024), doi:10.48550/arXiv.2407.10904, Submitted to Eur. Phys. J. C.

[4] ATLAS Collaboration, *Observation of Higgs boson production in association with a top quark pair at the LHC with the ATLAS detector*, Phys. Lett. B **784**, 173 (2018), doi:10.1016/j.physletb.2018.07.035.

[5] CMS Collaboration, *Observation of $t\bar{t}H$ production*, Phys. Rev. Lett. **120**(23), 231801 (2018), doi:10.1103/PhysRevLett.120.231801.

[6] LHC Higgs Cross Section Working Group, *Handbook of LHC Higgs Cross Sections: 4. Deciphering the Nature of the Higgs Sector* (CERN-2017-002-M) (2017), doi:10.23731/CYRM-2017-002.

[7] ATLAS Collaboration, *Measurement of Higgs boson decay into b-quarks in associated production with a top-quark pair in pp collisions at $\sqrt{s} = 13$ TeV with the ATLAS detector*, JHEP **06**, 097 (2022), doi:10.1007/JHEP06(2022)097.

[8] CMS Collaboration, *Measurement of the $t\bar{t}H$ and tH production rates in the $H \to b\bar{b}$ decay channel using proton-proton collision data at $\sqrt{s} = 13$ TeV* (2024), doi:10.48550/arXiv.2407.10896, Submitted to JHEP.

[9] ATLAS Collaboration, *Studies of Monte Carlo predictions for the $t\bar{t}b\bar{b}$ process* (ATL-PHYS-PUB-2022-006) (2022), https://cds.cern.ch/record/2802806.

[10] A. Vaswani, N. Shazeer, N. Parmar, J. Uszkoreit, L. Jones, A. N. Gomez, L. Kaiser and I. Polosukhin, *Attention Is All You Need* (2017), doi:10.48550/arXiv.1706.03762.

[11] M. J. Fenton, A. Shmakov, T.-W. Ho, S.-C. Hsu, D. Whiteson and P. Baldi, *Permutationless many-jet event reconstruction with symmetry preserving attention networks*, Phys. Rev. D **105**, 112008 (2022), doi:10.1103/PhysRevD.105.112008.